

Application of susceptibility weighted imaging (SWI) for evaluation of draining veins of arteriovenous malformation: utility of magnitude images

Toshiteru Miyasaka · Toshiaki Taoka ·
Hiroyuki Nakagawa · Takeshi Wada ·
Katsutoshi Takayama · Kaoru Myochin ·
Masahiko Sakamoto · Tomoko Ochi · Toshiaki Akashi ·
Kimihiko Kichikawa

Received: 16 January 2012 / Accepted: 9 March 2012 / Published online: 17 May 2012
© Springer-Verlag 2012

Abstract

Introduction The current study evaluated the signal characteristics of susceptibility weighted imaging (SWI) of arteriovenous malformation (AVM), especially for draining veins. For this purpose, we identified the draining veins of the AVM on angiography and evaluated the signal on magnitude image for SWI (SWI-mag) and minimum intensity projection image (SWI-minIP).

Methods Subjects were 14 cases with angiographically proven AVM. SWI-mag, SWI-minIP, and time-of-flight (TOF) magnetic resonance angiography were acquired. For the draining veins of the AVM identified on angiography, we analyzed signal intensity on the images listed above, and classified it into hyperintensity (hyper), mixed intensity (mixed), hypointensity (hypo), and no visualization.

Results On the analysis of 27 angiographically proven draining veins, 19 draining veins were classified as hyper, 3 as mixed, 0 as hypo, and 6 as no visualization on SWI-mag. On TOF images, 21 draining veins were classified as hyper, 2 as mixed, 0 as hypo, and 4 as no visualization, while 6 draining veins did not show hyperintensity on TOF, and SWI-mag visualized 3 of these 6 veins as hyper.

Conclusion SWI-mag depicted most draining veins of AVM as hyperintensity. We speculate that this is mainly due to the higher concentration of oxygenated hemoglobin (oxy-Hb)

and inflow effect of the draining vein. SWI-mag seems to be useful in the analysis and follow-up for AVM as the signal on the image may reflect physiological status.

Keywords Susceptibility weighted image · Magnitude image · Arteriovenous malformation · Magnetic resonance imaging

Introduction

Diagnosis of cerebral arteriovenous malformation has become less invasive due to advances in computed tomography (CT) and magnetic resonance imaging (MRI) technologies. These modalities provide important information that can be used for treatment planning such as surgical resection, interventional procedures, radiation, and/or their combination. In addition to providing morphological information about the size, shape, and location of arteriovenous malformation (AVM), hemodynamic information including recognition of inflow arteries and outflow veins and flow speed are important for treatment planning [1, 2]. Digital subtraction angiography (DSA) is the gold standard for evaluating hemodynamic information. Magnetic resonance digital subtraction angiography (MR-DSA) is one option for evaluating hemodynamics of AVM. However, the spatial resolution is not sufficient for strict clinical use. Although CT angiography can provide good morphological and spatial information, temporal resolution is restricted due to radiation exposure.

Susceptibility weighted image (SWI), which uses a fully flow compensated, long echo, gradient echo scan to acquire

T. Miyasaka (✉) · T. Taoka · H. Nakagawa · T. Wada ·
K. Takayama · K. Myochin · M. Sakamoto · T. Ochi · T. Akashi ·
K. Kichikawa
Department of Radiology,
Nara Medical University,
840 Shijo-cho,
Kashihara, Nara 634-8522, Japan
e-mail: michy@altgo.net

images, can identify susceptibility differences between tissues [3–5]. On SWI sequences, images are constructed from magnitude images (SWI-mag), which have a high resolution and long TE gradient echo image with flow compensation, and phase image, in which a high-pass filter is applied and used for making the phase mask. A phase mask processed from the phase image is applied to the magnitude image, and finally, minimum intensity projection is applied to emphasize low signal structures such as cerebral veins.

In general, the draining vein of an AVM contains a larger amount of oxy-Hb compared with a normal vein and is referred to as a “red vein” [6]. Theoretically, because draining veins of AVM have less susceptibility and higher flow speed, these veins are expected to show a high signal, such as arteries on SWI-mag. Although one report mentioned a high signal at the draining vein of AVM, no report has compared SWI-mag with DSA [7]. The purpose of this study is to evaluate signal characteristics of SWI for AVM, including original unprocessed magnitude images, especially for visualization of draining veins. For this purpose, we identified the feeding artery, nidus, and draining veins of AVM patients by using DSA and evaluated the signal characteristics of SWI-mag and SWI-minIP. We also evaluated the source image of time-of-flight magnetic resonance angiography (TOF-MRA).

Materials and methods

This retrospective study consists of consecutive patients in which MRI examination including SWI and DSA were performed from January 2006 to March 2011 in our institute. Written informed consent for the imaging study, including DSA, was obtained from all patients after the nature of the procedure was fully explained. Subjects consisted of 14 patients with angiographically proven AVM (9 males, 5 females; mean age, 47.6 years; range, 19–67 years). Symptoms included hemorrhage (eight patients), seizure (two patients), hemianopsia (one patient), headache (one patient), and two asymptomatic patients. The sizes of the AVM were less than 3 cm in 12 patients and 3 to 6 cm in 2 patients. Spetzler–Martin grades were 1 point in four patients, 2 points in five patients, 3 points in four patients, and 4 points in one patient. These patients were treated by embolization using an interventional procedure in one patient, a combination of embolization and surgical resection in two patients, a surgical procedure in five patients, and radiation therapy in two patients. Four patients were not treated and course watching was selected. The interval of MR imaging and DSA was within 1 month with the exception of two patients. In one of them, the interval was 10 months, and in the other, the interval was 6 months.

DSA was performed on bi-plane equipment (Digitex-2400, Shimadzu Medical System, Kyoto, Japan). Using the Seldinger technique from the common femoral artery, a 5-French diameter catheter was selectively positioned in the internal carotid artery or vertebral artery. Then, selective angiographies were acquired using 6 ml of contrast agent (Iopamiron 300, Schering AG, Germany) at a rate of 4 ml/s. Images were obtained with 1,024×1,024 matrix and 2.5 frames/s.

MR images were acquired using a 1.5-T clinical scanner (Magnetom Avanto, Siemens AG, Erlangen, Germany), and the protocol included the following sequences: (1) SWI (velocity compensated gradient echo sequence TR=49 ms, TE=40 ms, FOV=256 mm, imaging matrix=256×256, slice thickness=1.6 mm) and (2) TOF image (flash sequence TR=34–36 ms, TE=7.15 ms, FA=25, FOV=20 cm, matrix=320×320, slice thickness=0.65 mm). In addition of SWI and TOF-MRA, our protocol included axial image of T1-weighted imaging and T2-weighted imaging, sagittal image of T1-weighted imaging, coronal image of T2-weighted imaging, and diffusion-weighted imaging. SWI-minIP was obtained automatically on console at MR suite to create minimum intensity projections over 12.8 mm. Image observations were made using a picture archiving and communication system viewer. SWI images including SWI-mag, SWI-minIP, and original images of TOF-MRA were observed.

First, we identified the feeding arteries, nidus, and draining veins of the AVM by analyzing the early arterial to late venous phases of DSA images. For items identified on DSA, we analyzed the following points: (1) signal on SWI-mag, (2) signal on SWI-minIP, and (3) signal on TOF image. Signals on these images were evaluated visually by the consensus of two neuroradiologists (TM, TT) as hyperintensity to white matter (hyper), mixed intensity (mixed), hypointensity to the white matter (hypo), or no visualization. Mixed intensity was defined as having both hyperintensity and hypointensity. In addition, we analyzed patients in which the draining vein did not show hyperintensity on TOF images and looked at the signal of the draining vein on SWI images.

Results

Findings on DSA images showed that the location of AVM was frontal in four patients, parietal in two patients, occipital in two patients, temporal in one patient, in the thalamus in one patient, in the lateral wall of the ventricle in one patient, and in the posterior fossa in three patients. Twenty-one feeding arteries were identified in total, with up to five arteries in one patient. Twenty-seven draining veins were

identified in total, with up to four draining veins in one patient (Figs. 1, 2, and 3).

For the analysis of feeding arteries, 17 of 21 arteries were classified as hyper (81.0 %), 1 as mixed (4.8 %), 2 as hypo (9.5 %), and 1 as no visualization (4.8 %) on SWI-mag. On SWI-minIP, no arteries were classified as hyper or mixed, 13 were classified as hypo (61.9 %), and 8 were classified as no visualization (38.1 %). On TOF images, 21 feeding arteries were classified as hyper (100 %) and none showed hypo, mixed, or no visualization (Fig. 4a).

The signal of the nidus was also analyzed on SWI-mag and 5 of 14 nidus were classified as hyper (35.7 %), 8 as mixed (57.1 %), 0 as hypo (0 %), and 1 as no visualization (7.1 %). On SWI-minIP, one nidus was classified as hyper (7.1 %), two as mixed (14.3 %), seven as hypo (50.0 %), and four as no visualization (28.6 %). On TOF images, in patients for which TOF images were acquired, 14 nidus were classified as hyper (100 %) and none showed hypo or no visualization (Fig. 4b).

In the analysis of the signal of the draining vein, 19 of 27 draining veins were classified as hyper (70.4 %), 2 as mixed (7.4 %), 0 as hypo (0 %), and 6 as no visualization (22.2 %) on SWI-mag. On SWI-minIP, no draining vein was classified as

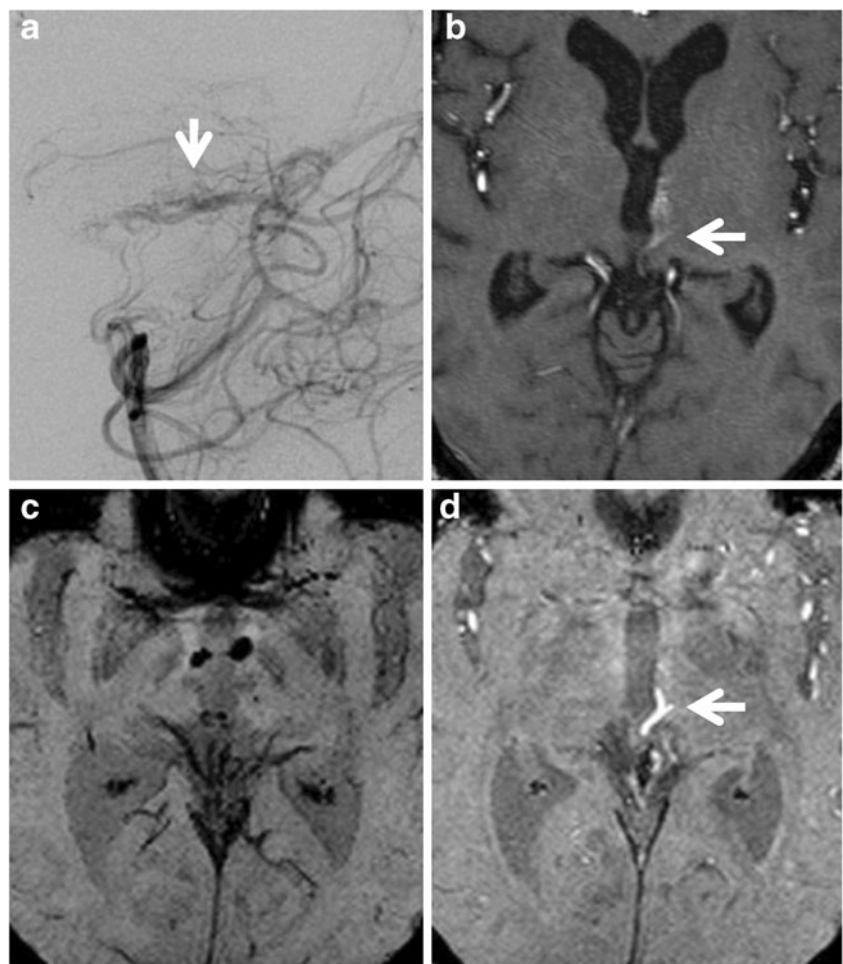
hyper (0 %), 0 as mixed (0 %), 10 as hypo (37.0 %), and 17 as no visualization (63.0 %). On TOF images, 21 draining veins were classified as hyper (77.8 %), 2 as mixed (7.4 %), 0 as hypo (0 %), and 4 as no visualization (14.8 %) (Fig. 4c).

There were six draining veins that did not show hyperintensity on TOF images including two mixed and four no visualization. The signal intensity of these six draining veins on SWI-mag was classified as hyper for three veins (50 %), mixed for one vein (16.7 %), hypo for zero vein (0 %), and no visualization for two veins (33.3 %). On SWI-minIP, no draining vein was classified as hyper (0 %), none as mixed (0 %), two as hypo (33.3 %), and four as no visualization (66.7 %) (Fig. 4d).

Discussion

AVM are congenital vascular lesions that consist of direct connections between arteries and veins, without an intervening capillary bed. Estimates of the prevalence of brain AVMs in the general population range from 0.5 to 1.8 per 100,000 population per year [8, 9]. The incidence of first-ever AVM hemorrhage is 0.51 per 100,000 population per

Fig. 1 A 41-year-old female patient with hemorrhagic AVM of the left thalamus. **a** Lateral view of the left vertebral angiography shows nidus and thick draining vein (*arrow*). **b** TOF image shows high signal intensity in the draining vein (*arrow*). **c** The draining vein is not clearly demonstrated on SWI (*arrow*). **d** Magnitude image presents high signal intensity in the draining vein (*arrow*)



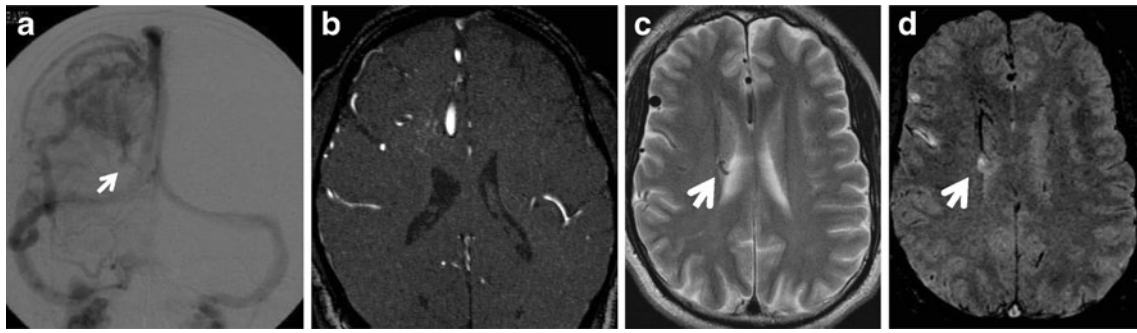


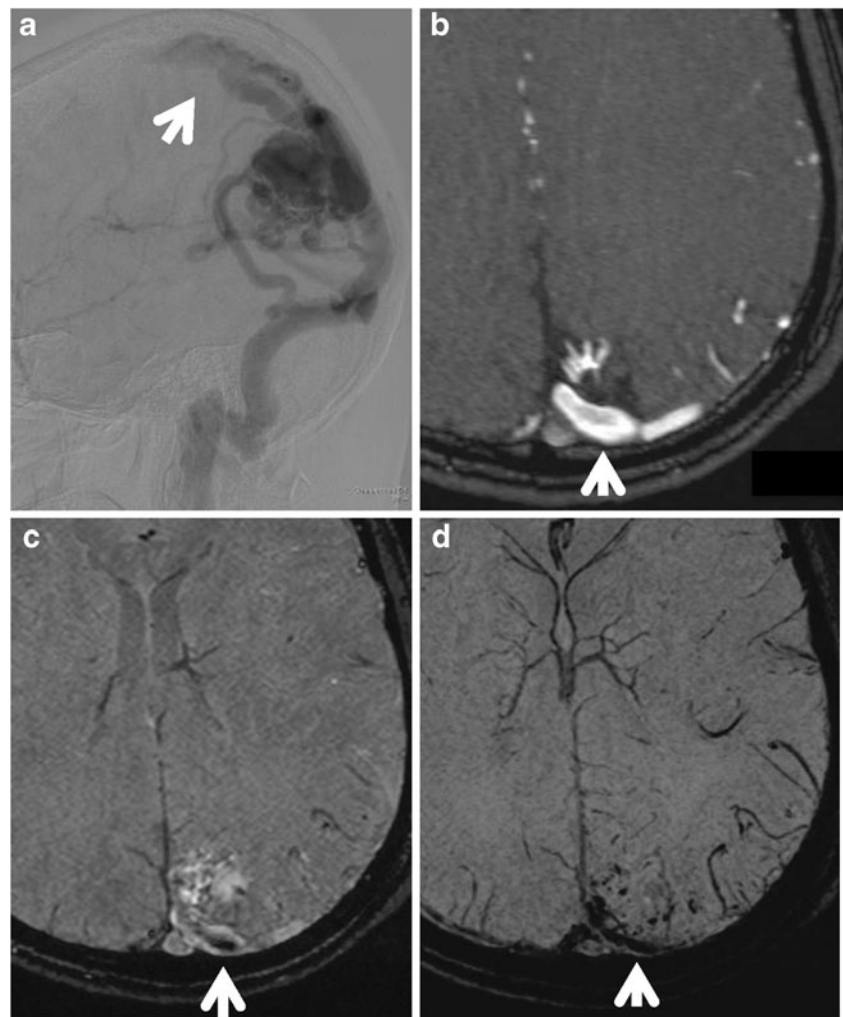
Fig. 2 A 39-year-old male with AVM in the right frontal AVM. Initial symptom was convulsion. **a** Right carotid angiography: nidus in the frontal lobe and several draining veins are visualized. Right thalamostriate vein (*arrow*) is one of the draining veins. **b** On the TOF image,

there is no visualization of the right thalamostriate vein. **c** T2-weighted image shows low signal flow void image of the right thalamostriate vein. **d** SWI-mag shows hyperintensity at the right thalamostriate vein

year [10]. Treatment for AVM includes surgical resection, embolization by interventional procedure, radiosurgery, or a combination of these methods [11, 12]. As interventional procedures and stereotactic radiosurgery methods have progressed, treatment strategies have been altered and some controversies have arisen [13]. Information about

the status of the draining vein, degree of shunt flow, existence of an aneurysm or varix, and size and location of the nidus are important for treatment selection. It is also important to evaluate the hemodynamics of the lesion during follow-up of patients [14]. DSA is still the gold standard for evaluation of AVM morphology and hemodynamics.

Fig. 3 A 53-year-old male patient with AVM in the left occipital lobe. **a** Venous phase of the left carotid angiography shows slow flow AVM with two thick and serpentine draining veins. **b** TOF image shows high intensity in the superficial cerebral vein. **c** Magnitude image shows mixed intensity. **d** SWI shows hypointensity



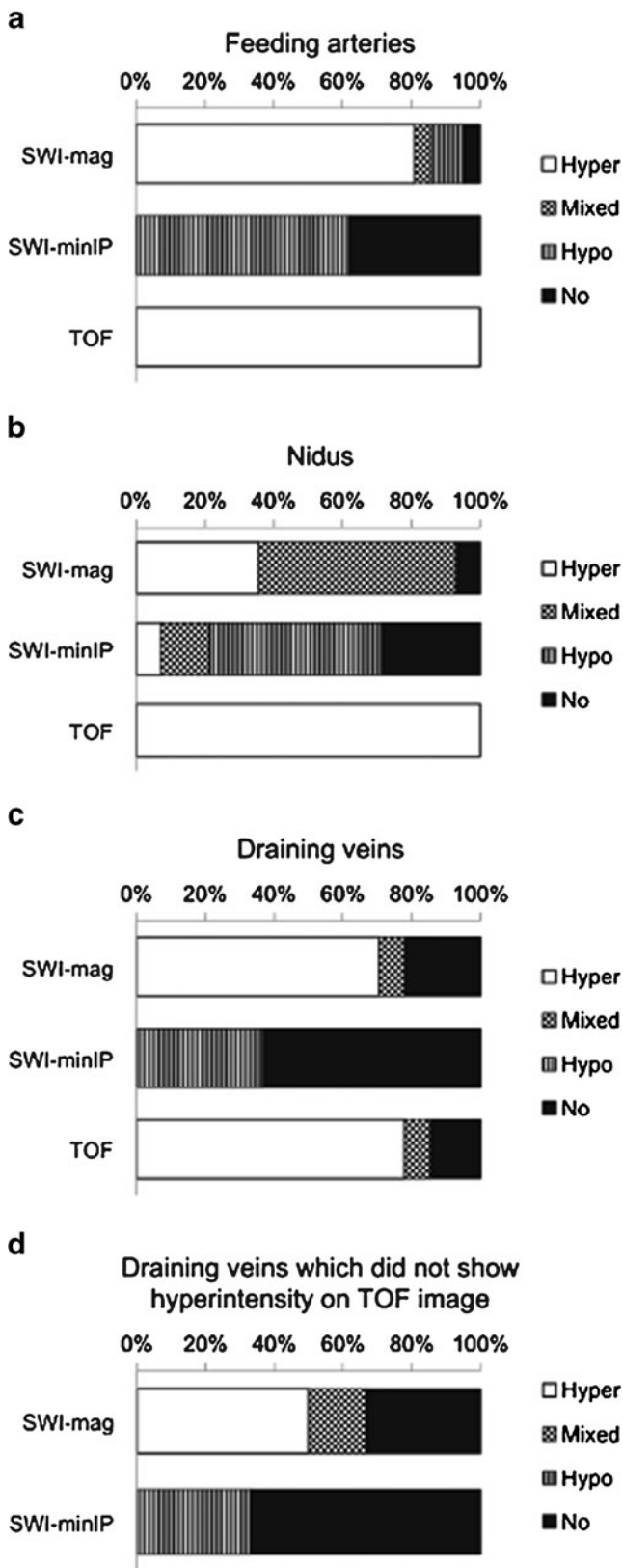


Fig. 4 a Visualization of the feeders on SWI and TOF images. All feeding arteries showed hyperintensity on TOF images due to high flow speed. On SWI-mag, 17 of 21 feeding arteries (81 %) showed hyperintensity. The hyperintensity of the feeding artery on SWI-mag may be due to high flow and high oxygen concentration of the arteries. b Visualization of the nidus on SWI and TOF images. The nidus also showed hyperintensity on TOF images in all patients. In contrast, a small number of nidus showed hyperintensity on SWI-mag and SWI-minIP. These were due to signal decreases due to bleeding within the nidus in most patients. c Visualization of the draining veins on SWI and TOF images. In contrast to the feeding artery and nidus, 6 of 27 draining veins (22.2 %) did not show hyperintensity on TOF images. On SWI-mag, 19 draining veins were classified as hyper (70.4 %). d Signal intensity on SWI images of the draining veins which did not show hyperintensity on TOF image. Among these six draining veins that did not show hyperintensity on TOF in c, SWI-mag showed hyperintensity for three veins (50 %), mixed intensity for one vein (16.7 %), hypointensity for zero vein (0 %), and no visualization for two veins (33.3 %). When the flow speed of the draining vein is lower, the SWI-mag seems to have merit as it depicts the vein as hyperintensity while TOF does not depict the vein as hyperintensity

desirable, especially for repeated follow-ups. CT angiography has shown great potential [15]. Morphological information can be readily depicted and spatial resolution is sufficient. However, due to the problem of radiation exposure, the time resolution is restricted; thus, it is difficult to evaluate hemodynamics by CT angiography. MRA is a powerful tool for evaluating arterial structures of the brain. Both the feeding artery and the nidus are clearly depicted by TOF-MRA, and this method provides morphological information with high spatial resolution [16]. However, depiction of the draining vein is insufficient, and it is difficult to obtain hemodynamic information. Although MR-DSA allows for evaluation of hemodynamics by MRI, spatial resolution is not sufficient [17].

In the current study, TOF images generally depicted feeding arteries, the nidus, and draining veins with high signals. SWI-mag showed high signals on feeding arteries and most of the draining veins. Some patients were judged as having a mixed intensity, in which the margin of the vessel showed a higher signal and the center of the vessel showed a lower signal, possibly due to a dephasing effect caused by the long TE of the sequence and high flow of the vein. SWI-minIP showed feeding arteries, the nidus, and draining veins as uniformly having a low signal, making discrimination between arterial and venous structures difficult. It is because of inherent for the minimal intensity projection. In general, the draining vein showed a higher signal by TOF than SWI-mag; however, six veins did not show a high signal on TOF images and three of them were depicted as having a high signal on SWI-mag. For both the SWI-mag and TOF images, the existence of a hemorrhage was a major factor involved in the worsening visualization of these vessels.

SWI is an imaging technique that maximizes the sensitivity to susceptibility effects and has exquisite sensitivity to

However, the procedure is invasive and has some risk for side effects; thus, noninvasive or less invasive methods are

the venous vasculature, blood products, and changes in iron content. The sequence uses a gradient echo technique with post-processing that provides sensitive detection of paramagnetic effects by combining magnitude information and filtered phase information [3–5]. The SWI-mag is the source image of SWI, which is a 3D gradient echo sequence with a long TE, short TR, small flip angle, high resolution, and full velocity compensation. Thus, it is not a simple gradient echo T2*-weighted image. Although it has a long TE, the small flip angle suppresses the signal from the cerebrospinal fluid and the short TR suppresses the signal from the brain parenchyma. The full velocity compensation prevents the signal within vessels from decreasing due to a dephasing effect from a long TE. Thus, the arteries show a high signal on SWI-mag. In contrast, TOF images consist of a sequence that emphasizes the arterial signal by the inflow effect by using a short TE and adjusting transverse magnetization via a ramped radiofrequency pulse. As a result, an arterial high signal on TOF images primarily depends on the flow speed. At 1.5 T, depending on the concentration of deoxygenated hemoglobin (deoxy-Hb) and oxy-Hb, arterial blood has a T2* of about 200 ms, and venous blood (70 % saturated) has a T2* of about 100 ms due to the susceptibility effect from deoxy-Hb. On the SWI-mag, the high signal of the artery mainly depends on rephasing by velocity compensation gradients and high concentrations of oxy-Hb within the vessels that prevent the signal decrease via the susceptibility effect from deoxy-Hb. In the draining vein, the concentration of the oxy-Hb is higher than in normal veins and the flow speed is higher than in normal veins [18]. Thus, the draining vein shows high signal both on TOF image and the SWI-mag. In particular, when the flow speed of the draining vein is higher, the TOF images tends to depict the vein with a higher signal; however, when the flow speed of the draining vein is lower, the SWI-mag seems to have merit as it depicts the vein with a high signal. The advantages and disadvantages of SWI-mag, SWI-minIP, and TOF are summarized in Table 1.

SWI is useful to detect microbleeding [19]. However, on SWI-minIP, when there is microbleeding within the lesion, it is difficult to assess vascular anatomy, because

microbleedings, the feeding artery, and the draining vein are described as having a low signal. In addition, SWI-minIP is sensitive to hemorrhagic products, so a blooming effect may disturb observation of fine vessel structure. SWI-mag can be used as a complement to back up the resolution of the vascular anatomy without being severely disturbed by a strong susceptibility effect from microbleedings, as it is less sensitive to blooming. In addition, it brings unique information about oxygenation within the vein that can only be provided by this image. Theoretically, as mentioned above, the magnitude image can depict the draining vein better than the TOF image when the flow speed of the vein is slow. Although TOF can visualize a rather high flow draining vein due to its pulse design, the information mainly depends on flow speed, which is different from that obtained on SWI-mag. In that sense, TOF images and SWI-mag provide very different information and can be complementary in nature. In particular, for patients with slow shunt flow such as those patients after treatment by intravascular embolization, follow-up examination by TOF is difficult and DSA may be necessary. Information by SWI-mag may not change the selection of treatment in the clinical practice, since DSA is still the golden standard for evaluating the morphology and hemodynamics of the AVMs. However, the use of the SWI-mag can be useful in the follow-up study after treatment. Although slow shunts were often visualized poorly on TOF-MRA, SWI-mag could demonstrate draining veins of slow-shunted AVM as hyperintensity. Red vein, which is visualized as high intensity on magnitude images, is one of the good indicators of recurrence and progression.

The current study has some limitations, including a small number of patients. However, we could evaluate 24 draining veins from 11 patients, which covered various flow statuses. There were two patients in which interval of MR imaging and DSA was as long as 10 and 6 months. Another limitation is that we used DSA as the gold standard and tried to evaluate the draining vein identified by DSA. As a result, the group of draining veins evaluated does not contain veins that were depicted only on MRI. In addition, our statement

Table 1 The advantages and disadvantages of SWI-mag, SWI-minIP, and TOF

	Advantages	Disadvantages
SWI-mag	<ul style="list-style-type: none"> • Draining veins are visualized as hyperintensity 	<ul style="list-style-type: none"> • Discrimination of feeding arteries and draining veins is sometimes confusing
SWI-minIP	<ul style="list-style-type: none"> • Dilated veins are well depicted • A small amount of hemosiderin is emphasized 	<ul style="list-style-type: none"> • Feeding arteries are not visualized clearly • A large hemorrhage shows severe blooming • Feeding arteries and draining veins are not discriminated
TOF	<ul style="list-style-type: none"> • The feeding arteries, nidus, draining veins are depicted in detail 	<ul style="list-style-type: none"> • Discrimination of feeding arteries and draining veins is sometimes confusing

on the flow effects on SWI signal intensity is still speculative. We could not delineate the impact of turbulent flow and pulsation artifacts of veins with an arterial flow pattern due to the AV shunting.

We selected white matter as standard for comparison of the vessel signal in the current study, not the normal veins. One of the reasons of the selection is the difficulty in comparing signal intensity of the draining veins with the normal vein, since the signal of normal veins on SWI are not uniform. The other reason is that it is difficult to determine “normal” veins in AVM cases. In addition, the major reason for this selection is that the difference between the signal intensity of the draining veins and the surrounding structure is the most useful in pointing out the draining vein in the clinical practice.

In conclusion, magnitude images for SWI depict a large number of draining veins of AVM as hyperintensity, even when hyperintensity in draining veins cannot be visualized on TOF images. We speculate that this phenomenon is mainly due to the higher concentration of oxy-Hb and inflow effect of the draining vein. Thus, the hyperintensity of draining veins of AVM on magnitude image of SWI may reflect the pathophysiology of AVM and can be helpful in pretreatment workup and posttreatment follow-up, especially when the draining veins do not show hyperintensity on TOF image due to slow flow.

Conflict of interest We declare that we have no conflict of interest.

References

- Ogilvy CS, Stieg PE, Awad I, Brown RD Jr, Kondziolka D, Rosenwasser R, Young WL, Hademenos G (2001) AHA Scientific Statement: recommendations for the management of intracranial arteriovenous malformations: a statement for healthcare professionals from a special writing group of the Stroke Council, American Stroke Association. *Stroke* 32(6):1458–1471
- Yuki I, Kim RH, Duckwiler G, Jahan R, Tateshima S, Gonzalez N, Gorgulho A, Diaz JL, De Salles AA, Vinuela F (2010) Treatment of brain arteriovenous malformations with high-flow arteriovenous fistulas: risk and complications associated with endovascular embolization in multimodality treatment. *Clinical article. J Neurosurg* 113(4):715–722. doi:10.3171/2009.9.JNS081588
- Haacke EM, Xu Y, Cheng YC, Reichenbach JR (2004) Susceptibility weighted imaging (SWI). *Magn Reson Med* 52(3):612–618. doi:10.1002/mrm.20198
- Sehgal V, Delproposto Z, Haacke EM, Tong KA, Wycliffe N, Kido DK, Xu Y, Neelavalli J, Haddar D, Reichenbach JR (2005) Clinical applications of neuroimaging with susceptibility-weighted imaging. *J Magn Reson Imaging* 22(4):439–450. doi:10.1002/jmri.20404
- Haacke EM, Mittal S, Wu Z, Neelavalli J, Cheng YC (2009) Susceptibility-weighted imaging: technical aspects and clinical applications, part 1. *AJNR Am J Neuroradiol* 30(1):19–30
- Barnett GH, Little JR, Ebrahim ZY, Jones SC, Friel HT (1987) Cerebral circulation during arteriovenous malformation operation. *Neurosurgery* 20(6):836–842
- George U, Jolappara M, Kesavadas C, Gupta AK (2010) Susceptibility-weighted imaging in the evaluation of brain arteriovenous malformations. *Neurol India* 58(4):608–614
- Stapf C, Mast H, Sciacca RR, Berenstein A, Nelson PK, Gobin YP, Pile-Spellman J, Mohr JP (2003) The New York Islands AVM Study: design, study progress, and initial results. *Stroke* 34(5):e29–e33. doi:10.1161/01.STR.0000068784.36838.19
- Al-Shahi R, Bhattacharya JJ, Currie DG, Papanastassiou V, Ritchie V, Roberts RC, Sellar RJ, Warlow CP (2003) Prospective, population-based detection of intracranial vascular malformations in adults: the Scottish Intracranial Vascular Malformation Study (SIVMS). *Stroke* 34(5):1163–1169. doi:10.1161/01.STR.0000069018.90456.C9
- Stapf C, Labovitz DL, Sciacca RR, Mast H, Mohr JP, Sacco RL (2002) Incidence of adult brain arteriovenous malformation hemorrhage in a prospective population-based stroke survey. *Cerebrovasc Dis* 13(1):43–46
- Starke RM, Komotar RJ, Hwang BY, Fischer LE, Garrett MC, Otten ML, Connolly ES (2009) Treatment guidelines for cerebral arteriovenous malformation microsurgery. *Br J Neurosurg* 23(4):376–386
- Soderman M, Andersson T, Karlsson B, Wallace MC, Edner G (2003) Management of patients with brain arteriovenous malformations. *Eur J Radiol* 46(3):195–205
- Starke RM, Komotar RJ, Hwang BY, Fischer LE, Otten ML, Merkow MB, Garrett MC, Isaacson SR, Connolly ES Jr (2008) A comprehensive review of radiosurgery for cerebral arteriovenous malformations: outcomes, predictive factors, and grading scales. *Stereotact Funct Neurosurg* 86(3):191–199
- Geibprasert S, Pongpech S, Jiarakongmun P, Shroff MM, Armstrong DC, Krings T (2010) Radiologic assessment of brain arteriovenous malformations: what clinicians need to know. *Radiographics* 30(2):483–501
- Gupta V, Chugh M, Walia BS, Vaishya S, Jha AN (2008) Use of CT angiography for anatomic localization of arteriovenous malformation Nidal components. *AJNR Am J Neuroradiol* 29(10):1837–1840
- Tanaka H, Numaguchi Y, Konno S, Shrier DA, Shibata DK, Patel U (1997) Initial experience with helical CT and 3D reconstruction in therapeutic planning of cerebral AVMs: comparison with 3D time-of-flight MRA and digital subtraction angiography. *J Comput Assist Tomogr* 21(5):811–817
- Tsuchiya K, Katase S, Yoshino A, Hachiya J (2000) MR digital subtraction angiography of cerebral arteriovenous malformations. *AJNR Am J Neuroradiol* 21(4):707–711
- Divani AA, Lieber BB, Wakhloo AK, Gounis MJ, Hopkins LN (2001) Determination of blood flow velocity and transit time in cerebral arteriovenous malformation using microdroplet angiography. *Ann Biomed Eng* 29(2):135–144
- Iwamura A, Taoka T, Fukusumi A, Sakamoto M, Miyasaka T, Ochi T, Akashi T, Okuchi K, Kichikawa K (2012) Diffuse vascular injury: convergent-type hemorrhage in the supratentorial white matter on susceptibility-weighted image in cases of severe traumatic brain damage. *Neuroradiology*. doi:10.1007/s00234-011-0892-9